ELSEVIER

Journal of Alloys and Compounds 230 (1995) 16–22

Journal of ALLOYS AND COMPOUNDS

Structure refinement and magnetic behaviour of the only selenide in the olivine group family: Mn_2SiSe_4

S. Jobic, F. Bodénan, P. Le Boterf, G. Ouvrard

Institut des Matériaux de Nantes, Laboratoire de Chimie des Solides, UMR 110, 2 rue de la Houssinière, 44072 Nantes Cédex 03, France

Received 21 April 1995; in final form 15 May 1995

Abstract

Mn_2SiSe_4 has been synthesized at 800°C. This compound cristallizes in the olivine-type structure with the cell parameters $a = 13.3066(8)$ Å, $b = 7.7780(5)$ Å and $c = 6.2451(3)$ Å in the *Pnma* space group. To date this structure type had been only reserved for oxides and sulfides. We report here the crystal structure determination of the first selenide with olivine structure. The magnetic measurements from 5 K to room temperature suggest the existence of preponderant antiferromagnetic interactions.

Keywords: Manganese; Selenide; Olivine

1. Introduction

During the last thirty years considerable research activity has been devoted to understanding the magnetic properties of low dimensional transition metal compounds. Among them the chalcogenides have played an essential role [1,2]. The chalcogenophosphates of general formula MPX_3 allowed the extension of the lamellar chalcogenide family towards the right side of the periodic table. More recently we obtained true lamellar chromium ternary tellurides $CrSiTe_3$ and $CrGeTe_3$ [3,4] in which the low dimensionality and the interesting magnetic properties of chromium chalcogenides occur together. These phases order ferromagnetically below 33 K and 61 K, respectively [4,5]. An intense synthesis activity led us recently to obtain new ternary chalcogenides: $CrSbSe_3$ [6], $CrSbS_3$ [7], and two different structural forms of $Cr_2Sn_3Se_7$ [8,9]. In parallel with the quest for new chromium low dimensional derivatives we were looking for other transition metal chalcogenides. After the work of Gopalakrishnan et al. on silicoselenides [10] we investigated the Mn–Si–Se system and obtained Mn_2SiSe_4, which is mentioned in the literature as being the only transition metal selenide with the olivine type structure [11]. This paper describes its detailed structure and magnetic behaviour at low temperature.

2. Experimental

The new phase appeared first as a subproduct of the reaction between 1Mn, 2Si and 4Se at 800°C for 2 weeks. Semi-quantitative scanning electron microscopy analyses were performed on single crystals and revealed the presence of the three elements. Accurate composition determination was not possible by this technique because of the lack of suitable standards but preliminary Bragg and Weissenberg photographs suggested that this phase was isostructural with Mn_2SiS_4 [12].

According to this hypothesis on chemical composition, the pure phase was then obtained by heating the elements in stoichiometric proportions (2:1:4) at 800°C (manganese, Koch-Light, 99.9%; silicon, Aldrich, 99%; selenium, Aldrich, >99.99%) in an evacuated silica sealed tube. The heating was performed at a rate of 10°C h^{-1} up to 800°C for 15 days, before cooling to room temperature at 20°C h^{-1}. The bulk is dark-brown, and tiny yellow crystals were observed in small amount. The presence of a small amount of α-MnSe impurity has been detected by X-ray powder diffraction.

Single crystals of Mn_2SiSe_4 were sorted from a batch obtained through the aforementioned procedure. A small yellow plate ($0.005 \times 0.050 \times 0.120$ mm^3) was glued on the top of a Lindeman fiber. Preliminary

0925-8388/95/$09.50
SSDI 0925-8388(95)01892-1

Bragg and Weissenberg photographs showed an orthorhombic cell with parameters $a = 13.15$ Å, $b = 7.66$ Å, and $c = 6.18$ Å, and revealed the existence conditions $0kl$ $k + l = 2n$ and $hk0$ $h = 2n$, in agreement with the space groups *Pnma* and $Pn2_1a$. Accurate parameters were determined by least-square refinement from data collected on a CPS 120 INEL X-ray powder diffractometer using monochromatized radiation Cu K-L_{III} ($\lambda = 1.54059$ Å) and equipped with a position-sensitive detector calibrated with $Na_2Ca_3Al_{12}F_{14}$ as standard. The refinement of the diagram, using a least-squares program [13] in the 10–101° 2θ range yields $a = 13.3066(8)$ Å, $b = 7.7780(5)$ Å, and $c = 6.2451(3)$ Å with an average 2θ angle deviation of 7/1000°. Table 1 shows the observed and calculated d spacings along with observed and calculated intensities [14]. The similarity of the cell parameters with those of Mn_2SiS_4 [12] and the space groups deduced from Weissenberg photographs suggest that the structures are isotypic, and that Mn_2SiSe_4 crystallizes in the olivine structure.

The crystal was transferred to an Enraf-Nonius CAD4 single-crystal X-ray diffractometer. Experimental parameters for the data collection and refinement are gathered in Table 2. After the usual corrections including Lorentz polarization and absorption correction by the Gaussian method ($\mu = 264.8$ cm^{-1}) and averaging according to the Laue symmetry Pmmm, a set of 424 independant reflections with $I > 3\sigma(I)$ was kept for structure refinement. All structure refinements and calculations were carried out with the XTAL3.2 structure determination package [15]. Conventional atomic and anomalous scattering factors were taken from the usual sources. The structure determination was carried out by comparison with the Mn_2SiS_4 olivine structure in the *Pnma* space group [12]. Final full matrix refinements yielded a reliability factor $R_F = 4.1\%$ ($R_{wF} = 2.9\%$) and a merit figure $S = 1.09$ for 41 refined parameters. Normal Atomic Displacement Parameters (ADP) are observed and the final difference electron density map did not reveal

Table 1
Observed and calculated d spacings in Å for Mn_2SiSe_4 and observed and calculated intensities determined from the Lazy Pulverix Program [14] (orthorhombic system, $a = 13.3066(8)$ Å, $b = 7.7780(5)$ Å, $c = 6.2451(3)$ Å, $V = 646.4(1)$ Å^3)

$h\,k\,l$	d_{obs}	d_{calc}	I_{obs}	I_{calc}	$h\,k\,l$	d_{obs}	d_{calc}	I_{obs}	I_{calc}
2 0 0	6.67	6.65	1	1	1 2 3	1.8185	1.8181	4	1
1 0 1	5.652	5.653	7	4	2 2 3	1.7695	1.7692	28	27
2 1 0	5.056	5.056	8	7	4 0 3	1.7646	1.7647	14	14
0 1 1	4.866	4.870	4	4	4 1 3	1.7204	1.7209	1	1
1 1 1	4.572	4.573	16	12	3 4 1	1.7126	1.7126	1	1
2 1 1	3.929	3.930	2	2	6 3 0	1.6856	1.6853	2	2
3 0 1	3.617	3.616	11	8	0 4 2	1.6507	1.6506	2	4
2 2 0	3.357	3.358	5	5	6 2 2	1.6394	1.6396	9	9
4 0 0	3.327	3.327	2	2	4 4 1	1.6213	1.6212	14	14
3 1 1	3.279	3.279	11	10	8 0 1	1.6070	1.6073	6	5
1 2 1	3.205	3.204	15	14	0 0 4	1.5614	1.5613	7	8
0 0 2	3.1237	3.1225	19	18	4 4 2	1.4786	1.4786	7	8
2 2 1	2.9575	2.9572	100	100	8 0 2	1.4681	1.4680	5	5
4 0 1	2.9362	2.9361	61	56	4 3 3	1.4588	1.4588	2	1
1 1 2	2.8319	2.8314	3	3	4 4 3	1.3068	1.3068	7	8
2 1 1	2.6565	2.6567	2	1	8 0 3	1.2992	1.2995	4	4
3 2 1	2.6475	2.6483	1	1	10 1 1	1.2839	1.2836	4	1
1 3 1	2.3569	2.3567	2	2	8 3 2	1.2774	1.2775	1	2
5 1 1	2.3363	2.3353	1	1	2 6 1	1.2470	1.2468	5	4
2 2 2	2.2868	2.2865	49	53	8 4 1	1.2390	1.2389	4	3
4 0 2	2.2772	2.2767	26	21	10 2 1	1.2342	1.2342	6	5
2 3 1	2.2538	2.2530	3	3	0 4 4	1.2174	1.2174	5	5
4 1 2	2.1853	2.1850	5	4	6 2 4	1.2129	1.2130	8	9
6 1 0	2.1330	2.1328	5	4	2 6 2	1.1782	1.1783	4	4
3 3 1	2.1074	2.1071	3	2	2 2 5	1.1708	1.1706	6	4
5 2 1	2.0719	2.0719	3	3	4 0 5	1.1693	1.1693	4	2
4 3 0	2.0454	2.0450	2	2	6 6 0	1.1189	1.1192	7	4
0 4 0	1.9444	1.9445	15	21	2 6 3	1.0856	1.0857	8	3
6 2 0	1.9265	1.9265	41	38	8 4 3	1.0803	1.0804	5	3
3 0 3	1.8846	1.8845	2	1	10 2 3	1.0772	1.0773	5	3
3 1 3	1.8314	1.8315	2	2	4 4 5	1.0020	1.0021	3	3
7 0 1	1.8185	1.8186	4	2					

Average 2θ angle deviation 7/1000°.

Table 2
Analytical and crystallographic data parameters of the X-ray data collection and refinement

Physical, crystallographic and analytical data
Formula Mn_2SiSe_4
Molecular weight 453.80 g mol^{-1}
Color yellow
Crystal symmetry orthorhombic Space group *Pnma*(62)
Cell parameters at room temperature refined from X-ray powder diagram
$a = 13.3066(8)$ Å, $b = 7.7780(5)$ Å, $c = 6.2451(3)$ Å
Volume $V = 646.4(1)$ $Å^3$
$Z = 4$
Density $\rho = 4.66$ g cm^{-3}
Absorption coefficient μ(Mo $K\text{-}L_{II\text{-}III}$) = 264.8 cm^{-1}
Crystal size $0.005 \times 0.050 \times 0.120$ mm^3

Data collection
Temperature 293 K
Radiation Mo $K\text{-}L_{II\text{-}III}$($\lambda = 0.71069$ Å)
Monochromator oriented graphite (0 0 2)
Scan mode ω/θ Scan angle $0.95 + 0.35 tg\theta$
Recording angle range 1.5°-35.0°
Standard reflections (−1 −4 −4), (1 4 4), (0 4 0)
Periodicity of intensity control 3600 s
Periodicity of orientation control 100 reflections
Absorption correction $abs_{min} = 1.133$; $abs_{max} = 3.288$

Refinement conditions
Investigated reciprocal space $-2 < h < 21$, $-2 < k < 12$, $-2 < l < 10$
Recorded reflections 2867
Independent reflections with $I > 3\sigma(I)$ 424
Refined parameters 41
Weighting scheme $1/\sigma(I)$

Refinement results
$R_F = 4.1\%$ $R_{wF} = 2.9\%$ $S = 1.09$
Extinction coefficient Ext(10000/G) = 0.006(1)
Difference Fourier intensity $+1.65$ $e^- Å^{-3}$, -2.21 $e^- Å^{-3}$

Table 3
Atomic coordinates and equivalent isotropic atomic displacement parameters

	x	y	z	B_{eq} (Å)
Mn(1)	0	0	0	1.34(8)
Mn(2)	0.2307(2)	1/4	0.5088(7)	1.03(8)
Si	0.4107(4)	1/4	0.0948(8)	0.71(8)
Se(1)	0.4073(2)	1/4	0.7353(4)	0.94(5)
Se(2)	0.5679(1)	1/4	0.2412(4)	0.96(6)
Se(3)	0.3318(1)	0.0203(2)	0.2508(3)	0.79(3)

Isotropic equivalent thermal factor defined as $B_{eq} = 4/3\Sigma_i\Sigma_j\beta_{ij}a_ia_j$.

meaningful extrema $(+1.65\ e^-\ Å^{-3}, -2.21\ e^-\ Å^{-3})$. Final values of the atomic parameters and anisotropic thermal parameters are summarized in Tables 3 and 4.

3. Structure description

The olivine structure can be described from a hexagonal close-packing of selenium atoms in the (*a,b*) plane. In such an AB stacking sandwich, manganese atoms occupy 1/2 of the octahedral sites while silicon atoms lay in 1/8 of the tetrahedra. Fig. 1 presents two adjacent chalcogen layers with the inserted cations.

The arrangement of ($MnSe_6$) octahedra in the (*a,b*) plane (Fig. 2) forms zig-zagging chains along the *b*-direction. The gap between adjacent chains has the same shape as the chains and is partially filled by silicon in tetrahedral coordination. The adjacent sheets are similar and shifted by $a/2$ in such a way that full and empty chains of octahedra alternate along *c*.

Such a metal-chalcogen arrangement defines two different manganese sites: (1) Mn(1), located at a center of symmetry, occupies all the octahedral sites along the *b*-axis either at $x = 1/2$ or $x = 0$, depending on the considered selenium sandwich, (2) Mn(2), located on a mirror plane perpendicular to [010], occupies 50% of the octahedra along the *b*-direction (octahedral sites at $x + 1/4$ and $x + 3/4$). So, in one layer Mn(1) atoms are always surrounded by two

Table 4
Anisotropic atomic displacement parameters

	U_{11}	U_{22}	U_{33}	U_{12}	U_{13}	U_{23}
Mn(1)	0.017(2)	0.015(2)	0.020(2)	0.003(1)	−0.002(2)	−0.002(2)
Mn(2)	0.012(1)	0.018(2)	0.011(2)	0	−0.004(2)	0
Si	0.009(3)	0.009(2)	0.010(3)	0	−0.004(3)	0
Se(1)	0.0117(8)	0.0145(8)	0.009(2)	0	−0.004(2)	0
Se(2)	0.0093(9)	0.0137(8)	0.013(2)	0	0.003(1)	0
Se(3)	0.0118(6)	0.0101(5)	0.008(1)	0	0.002(1)	−0.0000(9)

The expression of the general temperature factor is
$\exp[-2\pi^2(U_{11}h^2a^{*2} + U_{22}k^2b^{*2} + U_{33}l^2c^{*2} + 2U_{12}hkaa^*b^* + 2U_{13}hla^*c^* + 2U_{13}klb^*c^*)]$.

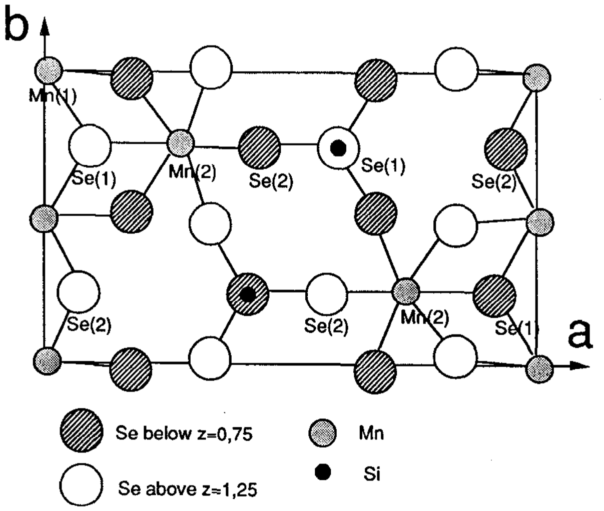

Fig. 1. Projection in the (*a*,*b*) plane of one AB selenium atom (large open shaded circles) stacking sheet sandwidching cations (manganese in spotted circle, and silicon in black circle) showing the labelling scheme. The non-labelled selenium atoms correspond to Se(3).

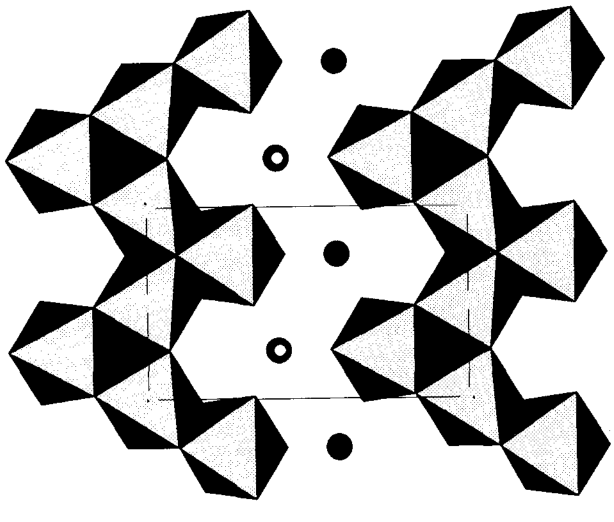

Fig. 2. Manganese octahedra in (*a*,*b*) plane defining [...Mn(1)–Mn(2)...] zigzagging entities along the *b*-axis.

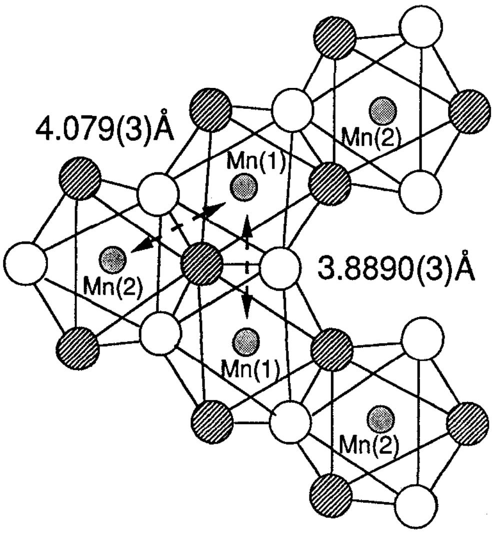

Fig. 3. Zig-zagging chains along the *b*-axis with the two different Mn–Mn distances.

Mn(1) and two Mn(2) atoms with two different Mn–Mn distances as shown in Fig. 3.

Fig. 4 shows the projection of the structure in the (*a*,*c*) plane and the zigzagging tunnels corresponding to the above-mentioned "vacant chains". In this tunnel, silicon atoms occupy tetrahedra whose one apex is the selenium atom common to three ($MnSe_6$) octahedra in the adjacent sheet.

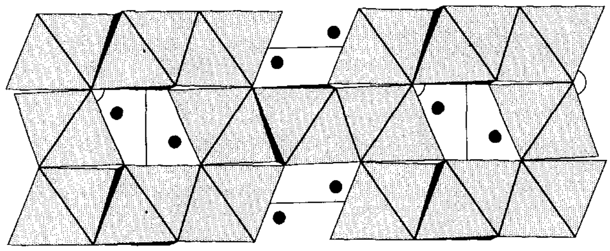

Fig. 4. Projection view in the (*a*,*c*) plane with black silicon atoms as black circles.

Table 5 gathers selected interatomic distances and angles related to the ($MnSe_6$) octahedra and ($SiSe_4$) tetrahedra. The Mn–Se distances agree with the sum of the van der Waals radii ($r_{\mathrm{MnIV}} = 0.83$ Å and $r_{\mathrm{Se-II}} = 1.98$ Å) [16] since the mean distances equal respectively 2.716(2) Å and 2.728(3) Å for Mn(1) and Mn(2) with low dispersions. Similar distances were observed in $MnPSe_3$ ($d = 2.72$ Å) [17]. Note, however, that the Mn(2)–Se(2) distance (2.671(4) Å) spreads out from the mean value to a greater extent than the five other Mn(2)–Se contacts. Moreover the shared Se–Se edges [Se(1)–Se(2) contacts between two successive Mn(1) octahedra, Se(1)–Se(3) contacts between Mn(1) and Mn(2) octahedra, and Se(2)–Se(3) and Se(3)–Se(3) contacts between Si tetrahedron and Mn(1) and Mn(2) octahedra respectively (see below)] are considerably shorter than the unshared edges. They range from 3.615(2) to 3.753(3) Å, and from 3.573(2) to 3.654(3) Å for (Mn(1)Se_6) and (Mn(2)Se_6) octahedra respectively, while the unshared edges go from 3.9067(4) to 4.060(3) Å, and from 3.815(3) to 4.205(2) Å. In addition, considering the *cis*-angles, the distortion of the Mn(1) octahedron appears less important than the distortion of that for Mn(2), which is in good agreement with the fact that the Mn(1) octahedra are in the heart of the chains and thus undergo a more symmetric stress field than those for Mn(2). In both cases the angles remain comparable with those found in the Mn_2SiS_4 olivine type structure [13].

Moreover, the ($SiSe_4$) tetrahedra show Si–Se distances in good agreement with the sum of van der Waals radii ($r_{\mathrm{SiIV}} = 0.26$ Å) [16] with a mean observed distance equal to 2.277(5)Å. This value is similar to the Si–Se distances calculated in $SiSe_2$ ($d_{\mathrm{Si-Se}} = 2.275$ Å). Nevertheless, as in the whole olivine type structure family, the ($SiSe_4$) tetrahedra are almost regular, with three longer chalcogen–main group element distances corresponding to edge shared Se(2) and Se(3) anions (2.283(6) and 2.290(4) × 2 against 2.246(6) Å), leading to an elongation of the polyhedron along the *c*-axis. The Se–Si–Se angles spread from the theoretical value (109.5°) with a rather wide dispersion since they go from 102.5° to 114.7°. As for the ($MnSe_6$) octahedra, the shared Se–Se edge distances are shorter (3.573(2)

Table 5
Mean interatomic distances (in Å) and angles (in °) with their estimated deviations

Mn(1) environment			
Mn(1)–Se(1)	2.731(2) × 2	*Mean distance*	
Mn(1)–Se(2)	2.685(2) × 2	Mn(1)–Se	2.716(2)
Mn(1)–Se(3)	2.731(2) × 2	Shared Se–Se	3.674(3)
		Unshared Se–Se	4.000(2)
Se(1)–Se(2)	3.753(3) × 2	Se(1)–Mn(1)–Se(1)	87.71(5) × 2
Se(1)–Se(2)	3.9067(4) × 2	Se(1)–Mn(1)–Se(1)	92.29(5) × 2
Se(1)–Se(3)	3.654(3) × 2	Se(1)–Mn(1)–Se(3)	83.98(6) × 2
Se(1)–Se(3)	4.060(3) × 2	Se(1)–Mn(1)–Se(3)	96.02(6) × 2
Se(2)–Se(3)	3.615(4) × 2	Se(2)–Mn(1)–Se(3)	87.74(6) × 2
Se(2)–Se(3)	4.033(3) × 2	Se(2)–Mn(1)–Se(3)	96.26(6) × 2
Mn(2) environment			
Mn(2)–Se(1)	2.742(4)	*Mean distances*	
Mn(2)–Se(2)	2.671(4)	Mn(2)–Se	2.728(3)
Mn(2)–Se(3)	2.720(3) × 2	Shared Se–Se	3.627(3)
Mn(2)–Se(3)	2.756(3) × 2	Unshared Se–Se	3.918(3)
Se(1)–Se(3)	3.654(3) × 2	Se(1)–Mn(2)–Se(3)	88.6(1) × 2
Se(1)–Se(3)	3.815(3) × 2	Se(1)–Mn(2)–Se(3)	83.31(9) × 2
Se(2)–Se(3)	3.940(2) × 2	Se(2)–Mn(2)–Se(3)	93.1(1) × 2
Se(2)–Se(3)	3.956(3) × 2	Se(2)–Mn(2)–Se(3)	94.40(9) × 2
Se(3)–Se(3)	3.573(2)	Se(3)–Mn(2)–Se(3)	80.8(1)
Se(3)–Se(3)	3.819(3) × 2	Se(3)–Mn(2)–Se(3)	88.45(5) × 2
Se(3)–Se(3)	4.205(2)	Se(3)–Mn(2)–Se(3)	101.3(1)
Si environment			
Si–Se(1)	2.246(6)	*Mean distances*	
Si–Se(2)	2.283(6)	Si–Se	2.277(5)
Si–Se(3)	2.290(4) × 2	Shared Se–Se	3.601(2)
		Unshared Se–Se	3.816(3)
Se(1)–Se(2)	3.814(3)	Se(1)–Si–Se(2)	114.7(3)
Se(1)–Se(3)	3.817(3) × 2	Se(1)–Si–Se(3)	114.6(2) × 2
Se(2)–Se(3)	3.615(2) × 2	Se(2)–Si–Se(3)	104.5(2) × 2
Se(3)–Se(3)	3.573(2)	Se(3)–Si–Se(3)	102.5(2)

and 3.615(2) × 2 Å) than the unshared edge distances (3.814(3) and 3.817(3) × 2 Å).

4. Discussion: olivine or spinel-type compounds $M_2^{II}AX_4$

Numerous olivine structure oxides and some sulfides have been previously studied as well as spinel structure compounds with the same formula $M_2^{II}AX_4$. These two structures differ in the chalcogen arrangement: hexagonal close-packing (olivine) or a cubic packing (spinel); the coordination of the cations remains identical but their partition in octahedra and tetrahedra is not the same. According to considerations on polyhedra size the olivine structure appears to be stabilized with rather small tetrahedrally coordinated ions and relatively large octahedrally coordinated ions, while the spinel structure will be stable in the opposite case.

The border limit is given by the ratio $(d_{M-X})_{mean}/(d_{A-X})_{mean}$ (or d_M/d_A) equal to $2/(3)^{1/2}$ (1.155) corresponding to the theoretical case of close packed spheres [18,19]. The olivine is stable above this limit and the spinel below it. The ratio d_M/d_A for Mn_2SiX_4 series (X = O, S, Se) decreases from 1.33 to 1.22 to 1.20 and explains the decrease of stability of the Mn_2SiX_4 olivine type. For comparison the ratio reaches 1.18 for Fe_2SiS_4 [19], a lower value than the 1.20 for Mn_2SiSe_4 . Hence the predicted d_M/d_A ratio of 1.18 for Mn_2SiTe_4 may suggest its synthesis in the olivine form.

In previous work on olivine oxides the distortion of the (MO_6) octahedra and the (AO_4) tetrahedra (A: main group element) was thoroughly discussed. It appears that the occurrence of repulsive electrostatic interactions between cations shortens the O–O bond of shared edges [19,20]. Hence the difference between the O–O bonds of occupied or unoccupied polyhedra leads to a large distortion.

In the sulfides the distortion is much smaller, even in Fe_2SiS_4 with non-symmetrical d^6 configuration of iron. The more covalent character of the bonds corresponding to a greater hybridization of metal and ligand orbitals decreases the distortion. With a more electropositive chalcogen the influence of electrostatic forces is weaker.

In the same way the first olivine type selenide tends also towards ideal hexagonal close packing. The d_{HS}^5 manganese configuration is probably related to the success in stabilizing selenide.

The greater density of the spinel structure has permitted experiments at high pressure and temperature on olivine structure oxides to determine the olivine–spinel border limits [21]. One could imagine the same transition in sulfides or selenide even if the experiment with Fe_2SiS_4 failed [18] and led to the destruction of the compound.

5. Magnetic properties

The powder X-ray diagram showed the presence of a small amount of the α-MnSe impurity. In order to reduce its presence a vapor transport reaction was achieved at 800°C with I_2 as transport agent. A collection of crystals of 10.00 mg were sorted.

Static magnetic measurements were performed using a Quantum Design SQUID magnetometer between 5 and 300 K. The magnetic behavior of Mn_2SiSe_4 in a 1 kG field, corrected from the diamagnetic contributions, is reported in Fig. 5.

For temperatures higher than 150 K the reciprocal susceptibility per manganese mole follows a Curie–Weiss law with a Curie constant of 4.365 emu K^{-1} mol^{-1} and a negative paramagnetic temperature $\theta_p = -230$ K. From the observed Curie constant an effective magnetic moment $\mu_{eff} = 5.91$ μ_B has been determined, in good agreement with a manganese d_{HS}^5 ($\mu_{theo} = 5.92$ μ_B with spin only contribution) expected from X-ray data and charge balance deduced from the stoichiometry. The negative θ_p value suggests the occurrence of predominant antiferromagnetic interactions at high temperature.

Below 150 K the inverse susceptibility goes down abruptly to 50 K then increases slightly to present a maximum at 25 K. Such magnetic perturbations cannot be explained by the α-MnSe still remaining: α-MnSe is an antiferromagnetic compound with a Neel ordering temperature of 140 K [22].

Similar (or simplest) magnetic behaviour has already been encountered for some olivine oxides and explained by spin arrangements which range from simple

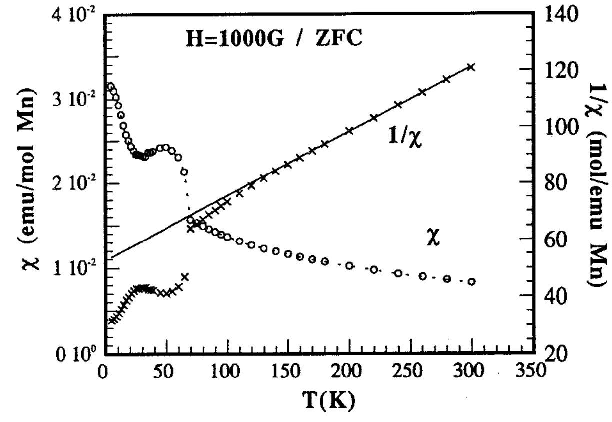

Fig. 5. Magnetic susceptibility per manganese mole after a zero field cooling of Mn_2SiSe_4 versus temperature in the 5–300 K temperature range.

colinear [23] to canted antiferromagnetism [24] and to complicated spirals [25,26].

Accurate magnetic susceptibility and neutron diffraction measurements are currently under way to explain this complex behaviour.

References

[1] P. Monceau (ed.), *Electronic Properties of Inorganic Quasi-one-dimensional Compounds; Physics and Chemistry of Materials with Low-dimensional Structures*, Series B, D. Reidel, Dordrecht, Holland, 1985.

[2] J. Rouxel (ed.), *Crystal Chemistry and Properties of Materials with Quasi-one-dimensional Structures; Physics and Chemistry of Materials with Low-dimensional Structures*, Series B, D. Reidel, Dordrecht, Holland, 1986.

[3] G. Ouvrard, E. Sandre and R. Brec, *J. Solid State Chem., 73* (1988) 27.

[4] V. Carteaux, D. Brunet, G. Ouvrard and G. André, *J. Phys: Condens. Mattter, 7* (1995) 68.

[5] V. Carteaux, G. Ouvrard, J.C. Grenier and Y. Laligant, *J. Magn. Magn. Mater., 5* (1991) 237.

[6] D. Odink, V. Carteaux, C. Payen and G. Ouvrard, *Chem. Mater., 5* (1993) 237.

[7] S. Jobic, P. Le Boterf, F. Bodénan and G. Ouvrard, *C.R. Acad. Sci. Paris, 318* (1994) 893.

[8] S. Jobic, P. Le Boterf and G. Ouvrard, *J. Alloys Comp., 205* (1994) 139.

[9] S. Jobic, F. Bodénan and G. Ouvrard, *J. Solid State Chem., 115* (1995) 165.

[10] J. Gopalakrishnan, K.S. Nanjundaswamy, *Mater. Res. Bull., 23* (1988) 107.

[11] V.G. Rocktäschel, W. Ritter and A. Weiss, *Z. Naturforsch., 19* (1964) 958.

[12] J. Fuhrmann and J. Pickardt, *Acta Crystallogr., C45* (1989) 1808.

[13] P. Deniard, M. Evain, J.M. Barbet and R. Brec, *Mater. Sci. Forum, 79* (1991) 363.

[14] R. Yvon, W. Jeitschko and E. Parthé, *J. Appl. Crystallogr., 10* (1977) 73.

[15] S.R. Hall, H.D. Flack and J.M. Stewart (eds.), *Xtal3.2 Reference Manual*, Universities of Western Australia, Geneva and Maryland, 1992.

[16] R.D. Shannon, *Acta Crystallogr., A32* (1976) 751.

[17] A. Louisy, *Thesis*, University of Nantes, 1981.

[18] B. Kamb, *Am. Min., 53* (1968) 1439.

[19] H. Vincent, E.F. Bertaut, W.H. Baur and R.D. Shannon, *Acta Crystallogr., B32* (1976) 1749.

[20] W.H. Baur, *Am. Min., 57* (1972) 709.

[21] A.D. Wadsley and A.F. Reid, *Acta Crystallogr., B24* (1968) 740.

[22] H. Heide, J.P. Sanchez and C.F. Bruggen, *J. Magn. Magn. Mater., 15–18* (1980) 1157.

[23] T. Duc, H. Vincent, E.F. Bertaut and V. Van Qui, *Solid State Comm., 7* (1969) 641.

[24] R.P. Santoro, R.E. Newnham and S. Nomura, *J. Phys. Chem. Solids, 27* (1966) 655.

[25] R.P. Santoro and R.E. Newnham, *J. Am. Ceram. Soc., 47* (1964) 491.

[26] D.E. Cox, B.C. Frazer, R.E. Newnham and R.P. Santoro, *J. Appl. Phys., 40* (1969) 1124.